Andreas H. Mahnken
Ernst Klotz
Anja Hennemuth
Bettina Jung
Ralf Koos
Joachim E. Wildberger
Rolf W. Günther

Measurement of cardiac output from a test-bolus injection in multislice computed tomography

A. H. Mahnken (✉) · B. Jung
J. E. Wildberger · R. W. Günther
Department of Radiology,
University Hospital,
Aachen University of Technology,
Pauwelsstrasse 52, 52074 Aachen,
Germany
e-mail: mahnken@rad.rwth-aachen.de
Tel.: +49-24-18088332
Fax: +49-24-18082499

E. Klotz · A. Hennemuth
Siemens Medical Solutions,
Forchheim, Germany

R. Koos
Medical Clinic I, University Hospital,
Aachen University of Technology,
Pauwelsstrasse 52, 52074 Aachen,
Germany

Abstract The aim of this study was to assess the feasibility of non-invasive determination of cardiac function from test-bolus data in multislice spiral computed tomography (MSCT). In 25 patients enhancement data gathered from a standardized test-bolus injection were analyzed. The test-bolus examination was performed prior to a retrospectively ECG-gated MSCT of the heart. A time–attenuation curve was obtained in the ascending aorta at the level of the pulmonary arteries. A gamma variate fit was applied to the curve in order to exclude recirculation and get pure first-pass data. Using the known amount of iodine injected, cardiac output (CO), and stroke volume (SV) were determined from integration of the fitted contrast nhancement curve using a reformation of the Stewart-Hamilton equation. Results were compared with CO and SV calculated from the geometric analysis of the retrospectively gated MSCT data using the ARGUS Software (Siemens, Forchheim, Germany). The CO and SV determined from test-bolus analysis and from geometric analysis correlated well with Pearson's correlation coefficients of 0.87 and 0.88, respectively. The standard deviation of the difference between both methods was 0.51 l/min for CO (8.6%) and 11.0 ml for SV (12.3%). Non-invasive quantification of CO seems to be feasible from a standard test-bolus injection. It provides valuable information on cardiac function without additional radiation or application of contrast material.

Keywords Computed tomography · Multi-detector row · Heart · Function

Introduction

The introduction of multislice spiral computed tomography (MSCT) scanners with four slices and 500 ms gantry rotation time in clinical routine led to an approximately eightfold increase of the examination speed and markedly improved temporal resolution, when compared with single-slice spiral CT with 1-s gantry rotation time [1]. Using retrospectively electrocardiogram (ECG)-gated MSCT allowed for the first time to perform CT coronary angiography [2, 3], motion-free evaluation of the entire thoracic aorta [4], and to quantitatively assess left ventricular volumes [5, 6, 7].

With the introduction of CT angiography, optimal timing of the contrast material injection became an important issue in CT. To achieve a more uniform contrast enhancement individually tailored injection protocols were developed [8, 9, 10]. For this reason the injection of a defined contrast material bolus and the subsequent acquisition of a low-dose time–attenuation curve prior to the actual spiral CT scan, a so-called test-bolus examination, is often performed. The primary aim of this examination is to determine the individual circulation time and from this the optimal time point for the start of the CT scan. As the time–attenuation curve after a defined bolus injection contains the cardiac system response, a test-bo-

lus examination is likely to hold quantitative information on cardiac function as well.

Applying a modification of the Stewart-Hamilton equation [11, 12], CT allows for the non-invasive measurement of CO. With the iodine contrast material as indicator and the CT scanner as densitometer animal experiments have shown previously that cardiac output (CO) can be determined from a defined contrast material injection and a dynamic measurement with electron beam tomography (EBT) or fast mechanical CT [13, 14, 15]. Patient studies on EBT comparing CO measured by indicator dilution vs geometric analysis from ECG-gated EBT showed systematic agreement but a high variability [16]. All these studies were performed using central-venous injection or even injection into the pulmonary artery, which cannot be considered non-invasive.

Therefore, the purpose of this study was to assess the feasibility of a non-invasive determination of CO with MSCT from routine test-bolus data after peripheral contrast injection as an adjunct to retrospectively ECG-gated MSCT of the heart.

Materials and methods

In 25 patients (16 men, 9 women) with a mean age of 64.8±13.2 years, who were referred to our clinic for exclusion of coronary artery disease (*n*=23), cardiomyopathy (*n*=1), or ventricular anomaly (*n*=1) retrospectively ECG-gated MSCT of the heart was performed. Patients suffering from valvular anomalies were excluded from the study. The average heart rate was 67.7±11.7 beats per minute (BPM). None of the patients received additional medication to reduce the heart rate prior the MSCT examination. In all patients informed consent was obtained. All MSCT examinations were performed with a four-detector-row MSCT scanner (Somatom Volume Zoom, Siemens, Forchheim, Germany).

Firstly, the circulation time was determined from a test-bolus injection. For this reason 20 ml of a nonionic contrast material (Ultravist 370, Schering, Berlin, Germany) followed by a saline chaser bolus of 30 ml were injected with a flow rate of 4 ml/s each. Contrast material was administered with an 18-G needle in the right cubital vein. After a start delay of 4 s, 20 sequential scans at the level of the pulmonary arteries were performed every 2 s during inspiratory breath-hold, resulting in a total scan time of 38 s. Scan parameters were chosen as follows: 4×2.5-mm collimation with a reconstructed slice thickness of 10 mm; 120-kV tube voltage with a tube current of 30 effective mAs; and a rotation time of 500 ms.

Secondly, the entire heart was examined during a single inspiratory breath-hold of 39.3±3.9 s duration. A standardized examination protocol with 4×1-mm collimation, 1.5-mm table feed per rotation (normalized pitch: 0.375), and a tube rotation time of 500 ms was used. Tube voltage was 120 kV with a tube current of 400 effective mAs. For vessel and ventricle enhancement 120 ml of a nonionic contrast material (Ultravist 370, Schering, Berlin, Germany) followed by a 50-ml saline chaser bolus were injected at a flow rate of 2.5 ml/s. The time-to-peak enhancement derived from the test-bolus examination multiplied by 1.5 was chosen as delay time. Radiation dose was calculated with a commercially available software (WinDose 2.1, Scanditronix Wellhöfer, Schwarzenbruck, Germany) [17].

For image reconstruction a field of view of 180×180 mm with a 512×512 reconstruction matrix and a soft tissue convolution kernel (B30f) were used. In each patient ten axial image series were reconstructed with an effective slice thickness of 1.25 mm and a reconstruction increment of 0.8 mm. Image series were calculated every 10% (0–90%) of the RR interval. The window settings were individually adapted for each examination using the half-contour principle [18]. The window center was set to the mean value of the density in the myocardium and the density in the ventricular lumen. Window width was defined as twice the window center. Temporal resolution of the image reconstruction algorithm was 125–250 ms, depending on the patient's heart rate [19].

The geometric analysis was performed on a workstation equipped with a standard software package (Wizard, Siemens, Forchheim, Germany). Standardized double-oblique multiplanar reformats in the short axis view were calculated from each axial image series [20]. For the reformatted images a slice thickness of 8 mm without slice gap was chosen as recommended by the Association of the Scientific Medical Societies in Germany (AWMF; http://www.uni-duesseldorf.de/WWW/AWMF/ll/dirad004.htm; accessed 6 April 2003). Using the multiplanar reformats end-systolic and end-diastolic images were selected by the reporting radiologist from the mid-portion of the left ventricle. End systole was defined as maximum contraction and end diastole as maximum dilatation of the left ventricle. Slices from the apex to the base were used for the quantitative assessment. The first slice with a visible lumen was defined as apex, whereas the base of the left ventricle was defined as the most basal slice with at least 50% myocardium [21]. Papillary muscles were excluded from the ventricular lumen as previously described [22]. The reformatted images were assessed using the ARGUS Software (Siemens, Forchheim, Germany) for analysis of cardiac function. From manually drawn endocardial contours of the left ventricle the stroke volume (SV) was calculated using Simpson's method (Fig. 1). The CO was calculated by multiplying the SV with the average heart rate of each patient; the latter was continuously recorded during the examination.

Time–enhancement curves were calculated for determination of CO from the test-bolus data. A region of interest (ROI) individually adjusted to the vessel size was placed in the ascending aorta. Contrast enhancement changes in the ROI were plotted against time utilizing a standard scanner function (DynEva, Siemens, Forchheim, Germany; Fig. 2). The time–enhancement curves were transferred to a separate computer equipped with a dedicated software tool for the calculation of CO based on the Stewart-Hamilton equation:

$$CO = \frac{Q}{\int_0^\infty c(t)dt} \qquad (1)$$

where Q is the amount of indicator injected and $c(t)$ is indicator-concentration as a function of time.

The Stewart-Hamilton equation assumes that the indicator enters the compartment just once and eventually completely leaves it. In order to restrict $c(t)$ to the first pass and to exclude re-circulation of the injected indicator from the analysis, a gamma variate function was fit to the time–enhancement curves before integration (Fig. 3) [23].

From previous studies and practical experience it can be assumed that part of the typical tail end of the bolus trails behind in the venous system and therefore a certain amount of the injected contrast material does not contribute to the measurement during the first pass [24]. As the calculation of CO is based on the fitted first pass of the contrast material exclusively, using the actually injected amount of contrast material in Eq. (1) will lead to an overestimation. To correct for this effect, the amount of tracer Q in the Stewart-Hamilton equation has to be replaced by an effective amount Q^*:

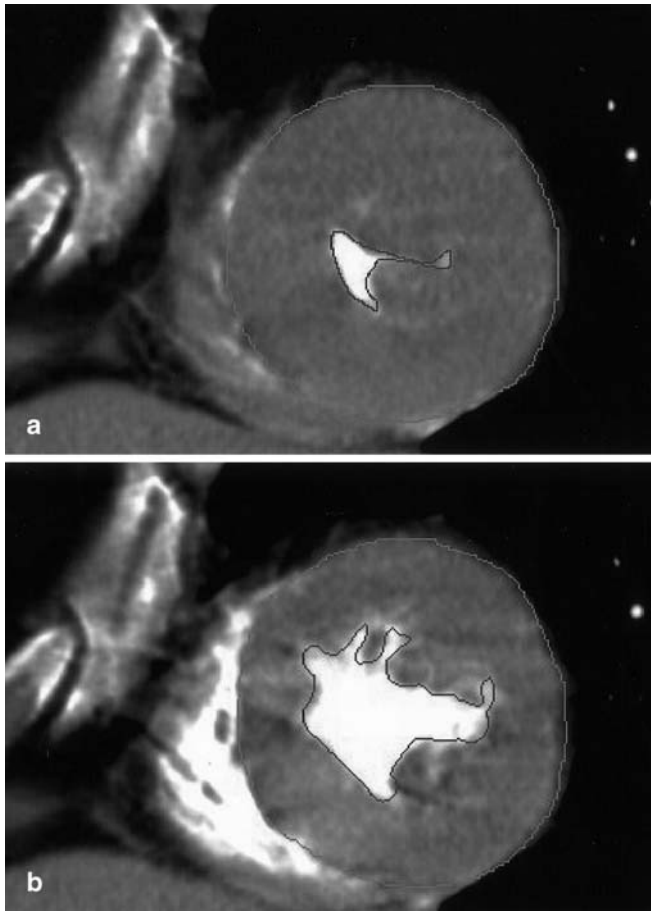$$CO = \frac{Q^*}{\int_0^\infty c(t)dt} \qquad (2)$$

Fig. 1a, b Multiplanar reformats in the short axis view in the **a** end-systolic and **b** end-diastolic phase allow for the calculation of the left ventricular volumes from manually drawn endocardial contours
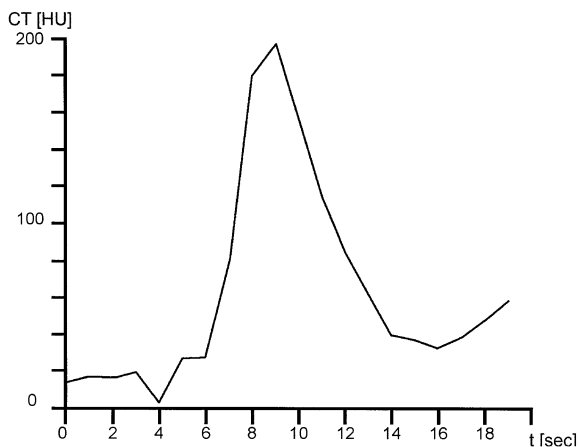

Fig. 2 Contrast enhancement changes in the ascending aorta were plotted against time, resulting in a time–enhancement-curve
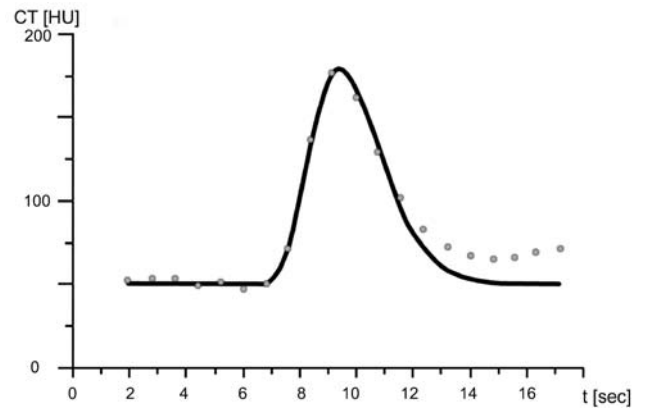

Fig. 3 In order to exclude re-circulation of the injected contrast material from the analysis, a gamma variate function was fit to the time–enhancement curves. The fitted curve is represented by the *black curve* with the *dotted curve* representing the original time–enhancement curve

with $Q* < Q$. The amount of contrast material trailing behind in the venous system is not exactly known, but if one assumes that it is relatively independent of CO and therefore a patient-independent constant, it can be estimated from the results by doing a proportionality fit to the data and by using the found proportionality constant as correction factor f_{corr} with $Q*=f_{corr}*Q$.

$c(t)$ in Eqs. (1) and (2) is a tracer concentration, specified, for instance, in milligrams of iodine per milliliter. The time–enhancement curve is measured as CT number (HU) and needs to be converted to tracer concentration units. With the well-known linear relationship of CT number and iodine concentration this can be achieved by a simple multiplication with a calibration constant. If is the CT-number change per unit of iodine concentration, and the area under the time–enhancement curve, then Eq (1) can be reformulated to:

$$CO = \frac{K * f_{corr} * Q}{A} \tag{3}$$

The conversion factor K was derived from a phantom study, measuring the CT number of several probes with a known amount of iodine. The slope of the resulting CT number–concentration relation was used as conversion factor K. The SV for the indicator dilution technique was calculated by dividing the CO by the patient's average heart rate during the test-bolus measurement.

Results of the geometric analysis of the MSCT data were compared with the results of the indicator dilution technique using regression analysis. Pearson's correlation coefficient was calculated. The agreement between both methods was assessed using the Bland-Altman approach [25].

Results

Multislice spiral CT examinations were successfully completed in all patients without complications. Breath hold during test-bolus injection and MSCT of the heart was maintained by all patients. The image quality was sufficient for quantitative image analysis in all examinations. Endocardial borders could easily be determined on
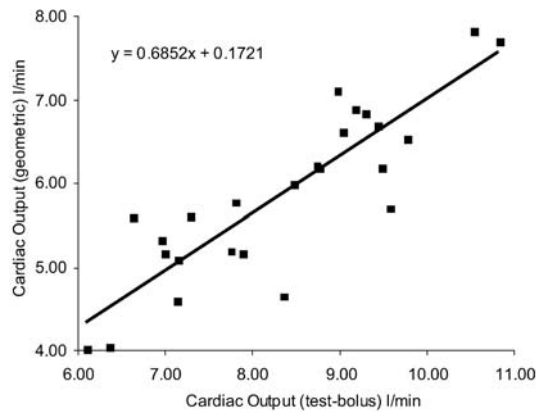
Fig. 4 Regression analysis shows good correlation between cardiac output (CO; l/min) determined from a geometric analysis of retrospectively ECG-gated MSCT of the heart and from test-bolus analysis. The analysis yields a regression line of $CO_{geom}=0.685{\times}CO_{test\text{-}bolus}+0.172$ l/min. The intercept of 0.172 is not significantly different from 0. This justifies the correction of the amount of tracer injected with a constant correction factor
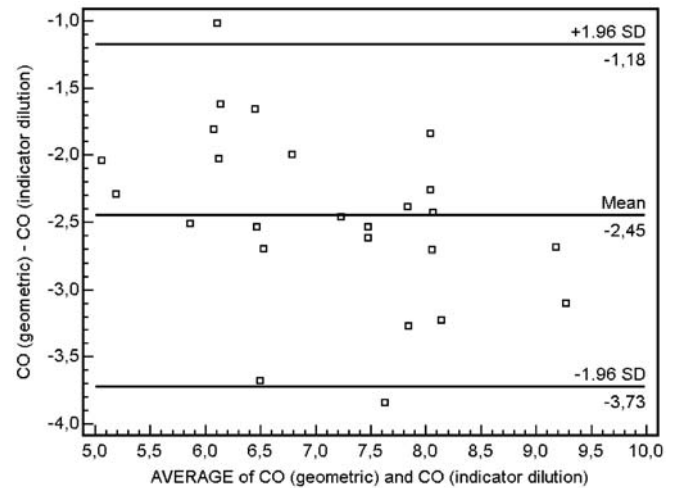

Fig. 5 Bland-Altman plot for the comparison with uncorrected test-bolus data shows a mean bias of −2.45 l/min for the CO. It also reveals that the difference between both methods considerably depends on CO

Table 1 Cardiac output (CO) and stroke volume (SV) determined by applying the indicator dilution theory to test-bolus data correlated well with geometric analysis. Results are given as mean±standard deviation before and after correction for trailing contrast material. In addition, the corresponding ranges of CO and SV are provided in parentheses

	Geometric analysis	Indicator dilution (Uncorrected)	Indicator dilution (Corrected)	Correlation Coefficient
CO (l/min)	5.88±1.02 (4.04–7.72)	8.33±1.33 (6.08–10.82)	5.91±0.92 (4.32–7.68)	0.87 −
SV (ml)	88.86±20.39 (51.9–148.4)	126.62±33.00 (79.89–207.95)	89.90±23.43 (56.72–147.64)	0.88 −

end-systolic and end-diastolic images. Left ventricular volumes calculated from the retrospectively ECG-gated MSCT data were as follows: end-systolic volume 72.3±106.1 ml; end-diastolic volume 166.3±104.4 ml; and ejection fraction 62.2±12.5%. Calculated effective radiation dose for the test-bolus injection according to ICRP 60 [26] was 0.74 mSv for men and 0.82 mSv for women. For ECG-gated MSCT of the entire heart the effective radiation dose was 6.87 mSv for men and 9.37 mSv for women.

The phantom measurements for determination of the conversion factor K show an excellent linear relationship between CT number and iodine concentration ($r^2=0.9995$) with a slope of 26.78 HU (mg iodine/ml).

Cardiac output and SV correlated well between both techniques with Pearson's correlation coefficients (r) of 0.87 and 0.88, respectively. The regression analysis of CO using the geometric method vs using the test-bolus method yielded a regression line of $CO_{geom}= 0.685*CO_{test\text{-}bolus}+0.172$ l/min (Fig. 4). The intercept of 0.172 l/min (95% confidence interval: −1.24 to 1.58 l/min) is not significantly different from 0. Setting the intercept to zero, the resulting correction factor for the contrast material not contributing to the first pass is 0.71. This corresponds to 5.8 ml of contrast material missing.

The results of CO and SV measurements for both techniques are summarized in Table 1. Bland-Altman analysis for the uncorrected data shows a mean difference of −2.45 l/min for the CO with limits of agreement ranging from −3.73 to −1.18 l/min (Fig. 5). The plot also reveals that the difference between both methods depends on CO. After application of the constant correction factor, the bias and size dependency of the difference is eliminated (Fig. 6). The corresponding mean differences for the SV before and after application of the correction factor are −37.8 (−1.0) ml with limits of agreement ranging from −2.8 (−22.7) ml to 72.7 (20.6) ml. The standard deviation of the difference in CO is 0.51 l/min, which corresponds to an average of 8.6%. The respective value for the difference in SV was 11.0 ml, corresponding to an average of 12.3%.
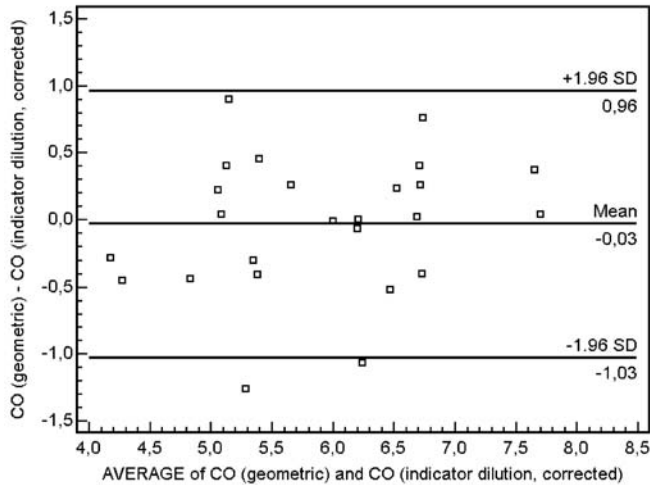
Fig. 6 After application of the constant correction factor, the bias and size dependency of the difference is eliminated. The standard deviation of the difference in CO is 0.51 l/min, which corresponds to an average of 8.6%

Discussion

Cardiac output is a parameter for the assessment of overall cardiovascular performance. Although CO is of limited use in clinical routine and more precise predictors of cardiac function, such as ejection fraction or end-diastolic volume, are commonly used, CO provides valuable information as a global parameter of cardiac function. Moreover, CO can be helpful to quantitate valvular insufficiencies and intra-cardiac shunts [27]; therefore, it can be of interest to determine CO as adjunct to a MSCT examination from otherwise unused CT data, without application of additional contrast material or radiation.

Several invasive and non-invasive methods to assess the CO are available, including thermodilution, radionuclide techniques, and ultrasound [28]. The CT allows assessing CO in different ways, firstly by a dynamic CT analysis using a modification of the indicator dilution method, and secondly by geometric assessment of the ventricular volumes from ECG-gated spiral CT data. Geometric analysis of the ventricular volumes in ECG-gated EBT and ECG-gated MSCT provided good results for the assessment of the cardiac function [5, 6, 7, 29, 30]. Indicator dilution technique was reported with very good results in animal studies [14, 15], and less satisfactory results in patient studies using EBT [16]. All these studies used a central venous line and very high flow rates for injection of the contrast material. To the best of our knowledge, the indicator dilution technique was not reported yet in patient studies using mechanical CT scanners and peripheral venous injection at a flow rate reasonable for standard CT examinations.

The Stewart-Hamilton equation requires the measurement of an indicator concentration in the blood pool to determine CO. Applying this to CT is fairly straightforward. Iodinated contrast material is used as indicator with the CT scanner employed as densitometer, measuring the CT number in a ROI. The CT number change is proportional to the change of the iodine concentration within the ROI. Repeated measurements at the same level result in a time–attenuation curve. To restrict the analysis to the first pass of the contrast material a gamma variate fit is applied. The exact relation between CT number and iodine concentration can be easily determined by scanning probes with known concentration of contrast material.

But there are several possible sources of error. The most important effect is caused by contrast material trailing behind in the venous system after injection of the test bolus. This phenomenon is caused by the dilution and slowing of the contrast material during the venous passage [10, 24, 31, 32]. Consequently, some of the contrast material arrives delayed at the heart and does not contribute to the analysis, as the calculation of the CO is based on a fitted first-pass exclusively. We corrected for this effect by introducing a patient-independent correction factor in Eq. (2). The fact that the intercept of the regression analysis was not significantly different from zero can be considered a retrospective justification for this assumption.

Right heart failure may result in a reflux of contrast material into the inferior vena cava, likewise resulting in an inaccuracy of CO determination. In case of a markedly prolonged circulation time the scan time for registration of the first pass of the contrast material might be too short to cover the entire contrast bolus increasing the error of the gamma variate fit. The influence of these effects is larger if only small amounts of contrast material are administered. They can be minimized by applying a saline chaser injection immediately following the injection of the contrast material.

For ionic and less so for nonionic contrast material hemodynamic and electrocardiographic changes were described [33, 34]. These effects are likely to be irrelevant for indicator dilution, as only small amounts of nonionic contrast material were injected, but they might possibly be relevant for the geometric analysis as this examination requires a much larger amount of contrast material. In addition, inspiratory breath hold leads to a decrease of the intrapulmonary pressure that may affect left ventricular filling; however, the type of breath hold should not influence the results of the study, as the test bolus injection as well as the ECG-gated MSCT of the heart were both performed using the same inspiratory breath hold.

To apply the indicator dilution technique to CT a sharply delineated test bolus is mandatory in order to receive a well-defined time–attenuation curve. This can be achieved by using a relatively fast injection rate. As in clinical routine the test bolus injection is used primarily

for determination of the circulation time, the flow rate of the test bolus injection has to be kept in reasonable agreement with the flow rate used for the diagnostic CT scan. In our study the circulation time determined from the test bolus injection was multiplied with the empiric factor of 1.5 in order to correct for the different flow rates. Another approach to solve this problem is to apply a biphasic scan protocol for the diagnostic CT scan with an initial flow rate of 4 ml/s as described elsewhere [35].

The geometric approach for determination of the cardiac function from retrospectively ECG gated MSCT has been shown to be quite accurate when compared with magnetic resonance imaging [6, 7, 30], which was established as gold standard for functional cardiac imaging [36]; however, geometric analysis of CT data sets showed a tendency to slightly underestimate the SV and therefore the CO. This effect is most likely caused by the limited temporal resolution of ECG-gated MSCT as motion free imaging of the heart requires a temporal resolution of 30–50 ms [37]. The reconstruction of only ten image series every 10% of the RR interval may also limit the determination of the left ventricular volumes, as the peak systolic contraction might be missed. In addition, the examined patient group consists mainly of patients with suspected coronary artery disease with only 2 patients suffering from other cardiovascular disorders.

All these factors may contribute to the differences observed between both techniques. Nevertheless, despite these potential limitations, there was good correlation and good agreement between both techniques. In comparison with previous animal and patient studies we found a systematic overestimation of the CO calculated from the time–attenuation curves. As discussed previously, this is most likely due to trailing contrast material arriving delayed at the heart. We were able to successfully correct for this effect by applying a constant correction factor which completely eliminated the systematic difference. In comparison with the patient study performed by Ludman et al. [16], our results showed a markedly reduced scattering of the data—by more than a factor of 2—indicating the applicability of this method in clinical routine by using modern MSCT scanners.

Conclusion

Non-invasive quantification of CO and SV is possible as a fast and simple additional post-processing procedure applied to standard test-bolus data. As a test-bolus injection is routinely used for determination of the circulation time in contrast-enhanced MSCT of the heart, this technique provides valuable information on the cardiac function without additional application of contrast material or radiation.

References

1. Klingenbeck-Regn K, Schaller S, Flohr T, Ohnesorge B, Kopp AF, Baum U (1999) Subsecond multi-slice computed tomography: basics and applications. Eur J Radiol 31:110–124
2. Ohnesorge B, Flohr T, Becker C, Kopp AF, Schoepf UJ, Baum U, Knez A, Klingenbeck-Regn K, Reiser MF (2000) Cardiac imaging by means of electrocardiographically multi-section spiral CT: initial experience. Radiology 217:564–571
3. Rodenwaldt J (2003) Multi-slice computed tomography of the coronary arteries. Eur Radiol 13:748–757
4. Flohr T, Prokop M, Becker C, Schoepf UJ, Kopp AF, White RD, Schaller S, Ohnesorge B (2002) A retrospectively ECG-gated multi-slice spiral CT scan and reconstruction technique with suppression of heart pulsation artifacts for cardio-thoracic imaging with extended volume coverage. Eur Radiol 12:1497–1503

5. Juergens KU, Grude M, Fallenberg EM, Opitz C, Wichter T, Heindel W, Fischbach R (2002) Using ECG-gated multi-detector CT to evaluate global left ventricular myocardial function in patients with coronary artery disease. Am J Roentgenol 179:1545–1550
6. Mahnken AH, Spuntrup E, Wildberger JE, Heuschmid M, Niethammer M, Sinha AM, Flohr T, Bücker A, Gunther RW (2003) Quantification of cardiac function with multi-slice spiral CT using retrospective EKG-gating: comparison with MRI. Fortschr Röntgenstr 175:83–88
7. Halliburton SS, Petersilka M, Schvartzman PR, Obuchowski N, White RD (2003) Evaluation of left ventricular dysfunction using multiphasic reconstructions of coronary multi-slice computed tomography data in patients with chronic ischemic heart disease: validation against cine magnetic resonance imaging. Int J Cardiovasc Imaging 19:73–83
8. Fleischmann D, Rubin GD, Bankier AA, Hittmair K (2000) Improved uniformity of aortic enhancement with customized contrast-medium injection protocols at CT angiography. Radiology 214:363–371

9. Kaatee R, van Leeuwen MS, de Lange EE, Wilting JE, Beek FJ, Beutler JJ, Mali WP (1998) Spiral CT angiography of the renal arteries: Should a scan delay based on a test-bolus injection or a fixed-scan delay be used to obtain maximum enhancement of the vessels? J Comput Assist Tomogr 22:541–547
10. Van Hoe L, Marchal G, Baert AL, Gryspeerdt S, Mertens L (1995) Determination of scan delay time in spiral CT angiography: utility of a test-bolus injection. J Comput Assist Tomogr 19:216–220
11. Herfkens RJ, Axel L, Lipton MJ, Napel S, Berninger W, Redington R (1982) Measurement of cardiac output by computed transmission tomography. Invest Radiol 17:550–553
12. Garrett JS, Lanzer P, Jaschke W, Botvinick E, Sievers R, Higgins CB, Lipton MJ (1985) Measurement of cardiac output by cine computed tomography. Am J Cardiol 56:657–661

13. Wolfkiel CJ, Ferguson JL, Chomka EV, Law WR, Brundage BH (1986) Determination of cardiac output by ultrafast computed tomography. Am J Physiol Imaging 1:117–123

14. Stewart GN (1897) Research on the circulation time and the influence which affects it. IV. The output of the heart. J Physiol 2:159–183

15. Hamilton WT, Moore JW, Kinsman JM, Spurling RG (1932) Studies on the circulation: further analysis of the injection method and of changes in hemodynamics under physiological and pathological conditions. Am J Physiol 99:534–551

16. Ludman PF, Coats AJ, Poole-Wilson PA, Rees RS (1993) Measurement accuracy of cardiac output in humans: indicator dilution technique vs geometric analysis by ultrafast computed tomography. J Am Coll Cardiol 21:1482–1489

17. Kalender WA, Schmidt B, Zankl M, Schmidt M (1999) A PC program for estimating organ dose and effective dose values in computed tomography. Eur Radiol 9:552–562

18. Thompson BH, Stanford W (1994) Evaluation of cardiac function with ultrafast computed tomography. Radiol Clin North Am 32:537–551

19. Flohr T, Ohnesorge B (2001) Heart rate adaptive optimization of spatial and temporal resolution for electrocardiogram-gated multi-slice spiral CT of the heart. J Comput Assist Tomogr 25:907–923

20. American Heart Association, American College of Cardiology, Society of Nuclear Medicine (1992) Standardization of cardiac tomographic imaging. From the Committee on Advanced Cardiac Imaging and Technology, Council on Clinical Cardiology, American Heart Association; Cardiovascular Imaging Committee, American College of Cardiology; and Board of Directors, Cardiovascular Council, Society of Nuclear Medicine. Circulation 86:338–339

21. Schalla S, Nagel E, Lehmkuhl H, Klein C, Bornstedt A, Schnackenburg B, Schneider U, Fleck E (2001) Comparison of magnetic resonance real-time imaging of left ventricular function with conventional magnetic resonance imaging and echocardiography. Am J Cardiol 87:95–99

22. Moon JC, Lorenz CH, Francis JM, Smith GC, Pennell DJ (2002) Breath-hold FLASH and FISP cardiovascular MR imaging: left ventricular volume differences and reproducibility. Radiology 223:789–797

23. Thompson HK, Starmer CF, Whalen RE, McIntosh HD (1963) Indicator transit time considered as gamma variate. Circ Res 14:502–515

24. Cademartiri F, van der Lugt A, Luccichenti G, Pavone P, Krestin GP (2002) Parameters affecting bolus geometry in CTA: a review. J Comput Assist Tomogr 26:598–607

25. Bland JM, Altman DG (1986) Statistical methods for assessing agreement between two methods of clinical measurement. Lancet 1:307–310

26. International Commission on Radiation Protection (1991) 1990 Recommendations of the International Commission on Radiation Protection. ICRP publication no. 60. Pergamon, Oxford

27. Kaminaga T, Naito H, Takamiya M, Nishimura T (1994) Quantitative evaluation of mitral regurgitation with ultrafast CT. J Comput Assist Tomogr 18:239–242

28. Botero M, Lobato EB (2001) Advances in noninvasive cardiac output monitoring: an update. J Cardiothorac Vasc Anesth 15:631–640

29. Baik HK, Budoff MJ, Lane KL, Bakhsheshi H, Brundage BH (2000) Accurate measures of left ventricular ejection fraction using electron-beam tomography: a comparison with radionuclide angiography, and cine angiography. Int J Card Imaging 16:391–398

30. Juergens KU, Fischbach R, Grude M, Wichter T, Fallenberg EM, Opitz C, Heindel WL (2002) Evaluation of left ventricular myocardial function by retrospectively ECG-gated multi-slice spiral CT in comparison to cine magnetic resonance imaging. Eur Radiol 12 (Suppl 1):S191

31. Platt JF, Reige KA, Ellis JH (1999) Aortic enhancement during abdominal CT angiography: correlations with test injections, flow rates, and patient demographics. Am J Roentgenol 172:53–56

32. Hittmair K, Fleischmann D (2001) Accuracy of predicting and controlling time-dependent aortic enhancement from a test-bolus injection. J Comput Assist Tomogr 25:287–294

33. Mancini GB, Bloomquist JN, Bhargava V, Stein JB, Lew W, Slutsky RA, Shabetai R, Higgins CB (1983) Hemodynamic and electrocardiographic effects in man of a new nonionic contrast agent (Iohexol): advantages over standard ionic agents. Am J Cardiol 51:1218–1222

34. Bettmann MA, Higgins CB (1985) Comparison of an ionic with a nonionic contrast agent for cardiac angiography: results of a multicenter trial. Invest Radiol 20:S70–S74

35. Kopp AF, Küttner A, Heuschmid M, Schröder S, Ohnesorge B, Claussen CD (2002) Multidetector-row CT cardiac imaging with 4 and 16 slices for coronary CTA and imaging of atherosclerotic plaques. Eur Radiol 12 (Suppl 2):S17–S24

36. Peshock RM, Willett DL, Sayad DE, Hundley WG, Chwialkowski MC, Clarke GD, Parkey RW (1996) Quantitative MR imaging of the heart. Magn Reson Imaging Clin N Am 4:287–305

37. Boyd DP, Lipton MJ (1983) Cardiac computed tomography. Proc IEEE Nucl Sci 71:298–307